Validation of a vector version of the 6S radiative transfer code for atmospheric correction of satellite data. Part I: Path radiance

Svetlana Y. Kotchenova, Eric F. Vermote, Raffaella Matarrese, and Frank J. Klemm, Jr.

A vector version of the 6S (Second Simulation of a Satellite Signal in the Solar Spectrum) radiative transfer code (6SV1), which enables accounting for radiation polarization, has been developed and validated against a Monte Carlo code, Coulson's tabulated values, and MOBY (Marine Optical Buoy System) water-leaving reflectance measurements. The developed code was also tested against the scalar codes SHARM, DISORT, and MODTRAN to evaluate its performance in scalar mode and the influence of polarization. The obtained results have shown a good agreement of 0.7% in comparison with the Monte Carlo code, 0.2% for Coulson's tabulated values, and 0.001–0.002 for the 400–550 nm region for the MOBY reflectances. Ignoring the effects of polarization led to large errors in calculated top-of-atmosphere reflectances: more than 10% for a molecular atmosphere and up to 5% for an aerosol atmosphere. This new version of 6S is intended to replace the previous scalar version used for calculation of lookup tables in the MODIS (Moderate Resolution Imaging Spectroradiometer) atmospheric correction algorithm.

OCIS codes: 280.1310, 290.4210, 010.1300, 010.1310, 010.1320, 120.0280.

1. Introduction

Natural light emitted from the Sun is not polarized. Before it enters the Earth's atmosphere, its intensity remains mostly unchanged and unaffected by the retardation of electric and magnetic components. However, after interacting with atmospheric molecules and particles, the unpolarized light may become partially polarized.[1–3] The degree of polarization depends on the type of scattering event. Incident radiation can be highly polarized (90%–100%) in a specific Sun sensor geometry due to an atmospheric effect such as Rayleigh scattering at a 90° scattering angle or a surface effect such as a sunglint in the specular direction. It usually becomes less polarized by small aerosol particles (~30%) or land surfaces such as snow (5%–25%), ice (0%–40%), sand (0%–15%), and vegetation (2%–23%).[1]

Accounting for radiation polarization requires the utilization of rigorous vector radiative transfer (RT) equations based on the Stokes parameters formalism.[1–3] In most cases, these equations are simplified by the assumption that the scattered radiation is not polarized and only the intensity of this radiation needs to be computed. Although this assumption has no physical background, it underlies a number of scalar RT codes, including DISORT (Discrete Ordinate Radiative Transfer),[4,5] MODTRAN (Moderate Resolution Atmospheric Transmittance and Radiance),[6] and SHARM,[7] which are widely used in different remote sensing applications related to the analysis and processing of satellite data.[8,9]

Numerous studies have been performed to evaluate and eliminate the errors induced by neglecting polarization in the case of a pure Rayleigh scattering. Van de Hulst[10] found that for certain angles the polarized light reflected by a finite Rayleigh atmosphere differed from the unpolarized one by more than 10%. Mishchenko *et al.*[11] rigorously examined large vector–scalar differences in the intensities of the radiation reflected by a homogeneous Rayleigh-scattering atmosphere for a wide range of incident and reflected light directions, single-scattering albedos, depolarization factors, optical thicknesses of the atmosphere, and surface reflectances. Lacis *et al.*[12] continued the study initiated by Mishchenko *et al.*[11] and further

S. Y. Kotchenova (skotchen@kratmos.gsfc.nasa.gov), E. F. Vermote, and F. J. Klemm, Jr., are with the Department of Geography, University of Maryland, 4321 Hartwick Road, Suite 209, College Park, Maryland 20740. R. Matarrese is with the Department of Physics, University of Bari, Via Amendola 173, Bari 70126, Italy.

Received 3 January 2006; revised 12 April 2006; accepted 14 April 2006; posted 17 April 2006 (Doc. ID 66885).

0003-6935/06/266762-13$15.00/0

investigated the magnitude and angular distributions of (scalar–vector)/vector relative errors caused by the scalar approximation for diffusely reflected and transmitted radiation. Diner *et al.*[13] incorporated a correction for radiation polarization in their RT algorithms used to generate the parameters of certain ancillary products and data sets required for processing of MISR (Multiangle Imaging Spectroradiometer) data. In particular, radiances calculated with a scalar code are corrected by subtracting the Rayleigh scattering contribution and replacing it with the contribution calculated by a vector code.

The effects of polarization for a pure aerosol atmosphere have not been studied that rigorously. To our knowledge, the range of publicly available RT codes capable of accounting for polarization in the case of an aerosol or mixed molecular–aerosol atmosphere is limited to the RT3 code[14] and those involving a Monte Carlo approach. However, there are a number of studies devoted to the retrieval of aerosol products from polarized radiation measurements. Bréon *et al.*[15] developed a retrieval algorithm for processing the spectral, directional, and polarized signatures of the Earth-reflected radiances measured by the POLDER (Polarization and Directionality of the Earth Reflectances) instrument over the land surface in the visible and near-infrared spectra. Mishchenko and Travis[16] retrieved aerosol characteristics, such as optical thickness, refractive index, and size distribution, from high-accuracy polarization and radiance measurements. Mishchenko *et al.*[17] investigated threshold science requirements for the Aerosol Polarimetry Sensor (APS), scheduled to fly on the NASA Glory mission, which would provide high-precision measurements of all four Stokes components in multiple spectral channels and at a number of viewing directions for the retrieval of aerosol major parameters. In general, these and similar studies are aimed at improving the current estimates of atmospheric aerosols performed with the help of passive remote sensing.

The errors resulting from ignoring the effects of light polarization can be crucial for the remote sensing studies dealing with efficient correction of atmospheric effects. An obvious illustration is satellite ocean-color monitoring,[18] which requires the ocean surface reflectance to be retrieved with an accuracy of 10^{-3}. Another example is the use of atmospherically corrected surface reflectances as inputs into other geophysical algorithms calculating vegetation indices[19] and net primary productivity[20] over the land surface. Any uncertainties in the inputs lead to larger uncertainties in the outputs. Thus, to obtain a good accuracy of RT computations, which underlie any atmospheric correction algorithm, it is necessary to elaborately consider the influence of polarization effects.

In this paper, we will present a new vector version of the 6S (Second Simulation of a Satellite Signal in the Solar Spectrum) code capable of accounting for radiation polarization in a mixed molecular–aerosol atmosphere and the results of its validation against other RT codes (scalar and vector) and ocean water-leaving reflectance measurements. We also provide an exhaustive study demonstrating the importance of the effects of polarization in RT modeling. This part of the study (Part I) is mainly focused on the atmospheric validation of the code; the assumption of a black (totally absorbing) surface is used in the majority of examples. The results of the validation involving the use of different surface bidirectional reflectance distribution functions (BRDF) will be provided in Part II.

2. Description of the New Version of 6S

The 6S code is a basic RT code used for calculation of lookup tables in the MODIS (Moderate Resolution Imaging Spectroradiometer) atmospheric correction algorithm.[21,22] It enables accurate simulations of satellite and plane observations, accounting for elevated targets, use of anisotropic and Lambertian surfaces, and calculation of gaseous absorption. The new vector version of the code can work in both scalar and vector modes. Hereafter, we will also refer to this new version as 6SV1.

The 6S code is based on the method of successive orders of scattering (SOS) approximations.[23] Within this method, the atmosphere is divided into a number of layers and the RT equation is solved numerically for each layer with the help of iterations. The intensity is successively computed for photons scattered one, two, three times, and etc. with the total intensity obtained as the sum of all orders. Numerical integration is performed using the decomposition in Fourier series for the azimuth angle and Gaussian quadratures for the zenith angle.

The effects of polarization are included through the calculation of four components of the Stokes vector, $\vec{I} = \{I, Q, U, V\}$. The first component, I, describes the intensity of radiation; the other three characterize perpendicular (Q), parallel (U), and elliptical (V) polarization. The degree, angle, and ellipticity of polarization are easily calculated from these last three components using simple mathematical formulas.[24] In the framework of the 3×3 approximation,[25] which is the case of 6SV1, $V = 0$. In scalar mode, $\vec{I} = \{I, 0, 0, 0\}$.

The Stokes parameters are specified in the coordinate system associated with the direction of propagation of incident light. To obtain their values with respect to the solar-viewer coordinate system, one should rotate them using the transformation matrix.[1,2] Changes of the Stokes parameters due to scattering events are calculated with the help of the molecular and aerosol phase matrices,[1–3] defined based on the Rayleigh and Mie scattering theories.

In addition to accounting for radiation polarization, several significant updates have been introduced into 6SV1. The updates include (i) a more accurate calculation of highly asymmetric aerosol scattering phase functions, (ii) an arbitrary variation of a vertical aerosol profile, (iii) the ability to change the number of calculation angles and layers, and (iv) the increase in the number of node wavelengths from 10 to 20.

In the previous version of 6S, the number of scattering angles at which a scattering phase function had to be specified was limited to 83. Since it was not enough for the calculations involving highly asymmetric aerosol scattering phase functions with large forwarding peaks, a special truncation procedure was applied to enhance the accuracy of phase function modeling in the case of large particles. Vertical distributions of aerosols were modeled using a default exponential profile with a maximum height of 2 km. RT simulations were performed using 48 calculation (Gaussian) angles and 26 calculation layers.

In the new version of 6S, there is an option to control the accuracy of phase function modeling by varying the number of scattering angles up to 1000. Six code-embedded aerosol models (continental, maritime, urban, desert, biomass burning, and stratospheric) are calculated using the default value of 83. A vertical aerosol profile can be specified arbitrarily by up to 50 layers in the height range from 0 to 100 km. There is also an option to improve the accuracy of RT simulations by increasing the number of calculation angles and layers.

The results presented in this study were obtained using 148 calculation angles and 50 calculation layers. Hereafter, this set of values will be referred to as the high-accuracy conditions. In general, the use of these conditions leads to an overall increase of the code accuracy of no more than 0.4%. The operational implementation of the other updates will also be demonstrated in this paper.

A ß version of the vector 6S (6SV1.0B) was released in May 2005 and can be downloaded through ftp://kratmos.gsfc.nasa.gov/pub/eric/6S. The manual for this version is currently in preparation. The user is advised to refer to the previous scalar version manual at ftp://kratmos.gsfc.nasa.gov/pub/6S/. We also provide a special Web interface that can help the inexperienced user learn how to use the code. The interface is available at http://6s.ltdri.org.

3. Validation Scheme

The new vector version of 6S has been validated against Coulson's tabulated values, other RT codes, and ocean water-leaving reflectance measurements. The validation scheme is presented in Fig. 1. We evaluated the performance of the code in both vector and scalar modes. Validation against the other codes was performed separately for molecular and aerosol atmospheres for a wide range of atmospheric, spectral, and geometrical conditions. Top-of-atmosphere (TOA) reflectances were calculated as outputs in the all RT codes.

In vector mode, the performance of 6SV1 was tested against Coulson's tabulated values for the case of a pure molecular atmosphere, against a Monte Carlo code for both molecular and aerosol atmospheres, and against ocean reflectance measurements for a mixed (aerosol plus molecular) atmosphere. Coulson's tabulated values were chosen for comparison as they represented the exact distribution of the reflected light in a plane-parallel atmosphere in accordance with Rayleigh's law. The Monte Carlo code was included as an integral part of the new code validation study. The ocean water-leaving reflectances were those measured by the MOBY (Marine Optical Buoy System) above the ocean surface near Lanai Island, Hawaii, in 2003.

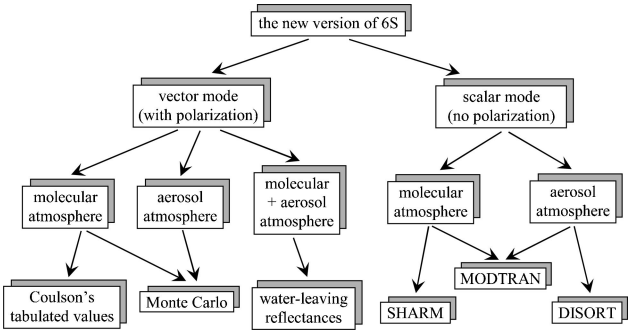

Fig. 1. Validation scheme of 6SV1.

In scalar mode, the performance of 6SV1 was tested against SHARM and MODTRAN for a molecular atmosphere and against MODTRAN and DISORT for an aerosol atmosphere. SHARM was chosen for comparison because of the results of the previously published comparison study,[7] where the relative accuracy of 6S compared to SHARM was stated to be 0.6% for a molecular atmosphere and 1%–2% for an aerosol atmosphere. The same study reported that the relative difference between the outputs of SHARM and the well-known code DISORT did not exceed 0.05% for both molecular and aerosol atmospheres for the view zenith angle (VZA) range of 0°–80°, except for the backscattering direction, where it suddenly increased to 0.5% for the aerosol atmosphere. This sharp increase in discrepancy was explained as having come from the single-scattering term, which was calculated differently in SHARM and DISORT. To avoid the appearance of the same problem in comparison between SHARM and 6S, the SHARM code was replaced by DISORT for the case of an aerosol atmosphere. MODTRAN was chosen for comparison for both molecular and aerosol atmospheres because of its popularity in the remote sensing community.

Short descriptions of each code and Coulson's tabulated values are provided in Section 4. Validation against these codes is described in Section 5. Effects of polarization are discussed in Section 6. Validation against the ocean reflectances is presented separately in Section 7.

4. Description of Other Codes

A. Vector Codes

Monte Carlo is a 3D RT code where one photon at a time is followed on its 3D path through the atmosphere starting from the moment of its emission.[26] Each photon is characterized by a statistical weight whose value is initially set to unity. Absorption and scattering events that may happen to the photon on its way through the scattering media change its statistical weight. The photon is considered terminated

when it emerges from the top of the atmosphere or when its statistical weight becomes less than a specially indicated minimum. The absorption and scattering processes are described by suitable probability functions. A Monte Carlo code is generally considered a benchmark for comparison with other RT codes because it does not have any limitations except for large amounts of calculation time and angular space discretization.

The code used in the present study is written based on the four-component Stokes vector approach. It is particularly designed to study polarized reflectance at the top of the atmosphere for various atmospheric and surface conditions.[15] One of its most common applications includes simulation of atmosphere–ocean interactions. The code is available from its author by request.

Coulson's tabulated values represent the complete solution of the Rayleigh problem for a molecular atmosphere.[27] The present set of tables gives the exact distribution and polarization of the reflected and transmitted light in a plane-parallel atmosphere scattering for a wide range of geometrical, surface boundary reflectance, and atmospheric optical conditions.[24] These values are truly considered a benchmark for everybody who is willing to validate a vector RT code.

B. Scalar Codes

SHARM is a 1D RT code designed to perform simultaneous computations of monochromatic radiance or fluxes in the short-wave spectral region for a large set of initial geometric conditions and multiple wavelengths.[7] The code is based on the method of spherical harmonics with an incorporated correction function technique of angular smoothing of solution.[28] Atmospheric properties can be varied arbitrarily in the vertical dimension. However, if users want to define several atmospheric layers with different types of aerosol, it is their responsibility to provide files containing aerosol scattering phase function values for each layer. The code has a routine to perform Mie calculations but only when the type of aerosol is the same for all layers. Also, calculation of gaseous absorption is not included in the code. The user is prompted to specify gaseous absorption as an input via absorption optical thickness values at the boundaries of each atmospheric layer. The code has mainly been tested against SHDOM[29] (Spherical Harmonic Discrete Ordinate Method) and DISORT.[4,5] It is publicly available at ftp://ltpftp.gsfc.nasa.gov/projects/asrvn/.

DISORT is one of the most heavily tested RT codes available for a plane-parallel atmosphere. It is based on the discrete ordinate method of radiative transfer, which enables time-independent calculations in a vertically inhomogeneous layered atmosphere. The simulated physical properties include thermal emission, scattering, gaseous absorption, and bidirectional surface reflection.[4,5] This code was designed to find numerous applications from the UV to the radar spectral region. It might be a little inconvenient to use in the case of a user-defined aerosol atmosphere, as the user is responsible for providing a full aerosol phase function Legendre expansion. The code is publicly available at ftp://climate1.gsfc.nasa.gov/wiscombe/Multiple_Scatt/.

MODTRAN is a 1D RT code most widely used for the analysis of AVIRIS (Airborne Visible/Infrared Imaging Spectrometer) data.[6] In addition to efficient modeling of scattered radiance and atmospheric attenuation, the code is able to simulate molecular and cloud–aerosol emission. It uses a spherically symmetric atmosphere, consisting of a number of homogeneous layers with a boundary specification of temperature, pressure, and atmospheric species concentration. The DISORT code is used as a subroutine in MODTRAN to enable implementation of the azimuth dependence of multiple scattering in each layer. The research presented in this paper was done using MODTRAN4, the latest publicly released version of the code[30,31] (available from its authors by request).

5. Validation of the Vector 6S against other Radiative Transfer Codes

A. Scalar Mode

1. Molecular Atmosphere

For a molecular atmosphere, the performance of the new version of 6S in scalar mode was tested against SHARM and MODTRAN. In both cases, the atmosphere was represented as a single molecular layer with the Rayleigh scattering phase function. The depolarization factor, describing the effects of molecular anisotropy, was turned off in 6S and MODTRAN. The main objective was to compare the performance of the radiative transfer bodies of the codes in the case of a symmetrical phase function. Any differences associated with the use of an asymmetric phase function would be revealed in the case of a purely aerosol atmosphere.

The comparison was done for six different values of the solar zenith angle (SZA), SZA = {0.0°; 10.0°; 23.07°; 45.0°; 58.67°; 75.0°} and three values of relative azimuth (AZ), AZ = {0.0°; 90.0°; 180.0°}. The VZA varied from 0° to 79° with an increment of 5° for one set of values; the other set included the values specified in Coulson's tables.[24] Four different wavelengths corresponding to the blue and red bands of the visible spectrum were chosen for the comparison. The background surface was assumed to be totally absorbing, $\rho = 0$.

In comparison with SHARM, the optical thicknesses calculated in 6SV1 ($\tau = 0.3445$ for 400 nm and $\tau = 0.1$ for 530 nm) were manually input into SHARM to avoid the inconsistencies associated with the use of different methods for optical thickness calculation. The results are presented in Fig. 2(a). SHARM was used as a reference to calculate relative percentage differences between the outputs of the codes. The absolute value of the maximum observed difference does not exceed 0.0125% for $\tau = 0.1$ and 0.015% for $\tau = 0.3445$. 6SV1 was also tested under

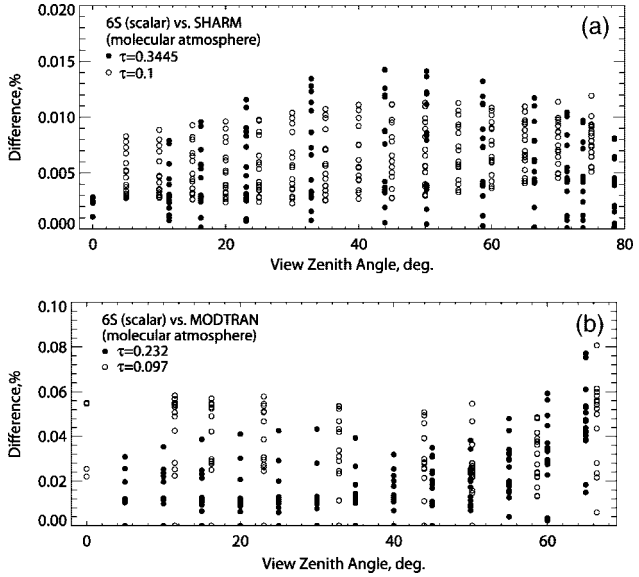

Fig. 2. Validation of 6SV1 in scalar mode against (a) SHARM and (b) MODTRAN for a molecular atmosphere. (a) SZA = {0.0°; 10.0°; 23.07°; 45.0°; 58.67°; 75.0°}, AZ = {0.0°; 90.0°; 180.0°}, VZA = {0°–79°}, optical thickness of τ = {0.1; 0.3445}, surface reflectance of $\rho = 0$. (b) SZA and VZA sets do not include angles beyond 70°, τ = {0.097; 0.232}, $\rho = 0$.

the standard accuracy conditions, used in the previous scalar version of 6S (the results are not presented here). The maximum observed difference did not exceed 0.3%, which was still notably lower than the accuracy of 0.6% reported in the previous comparison study.[7]

Agreement at larger values of optical thicknesses is a better indicator of the codes' consistency. The single scattering component of the reflected radiation—the term that can be expressed analytically—is dominant for $\tau = 0.1$, where it accounts for 78%–91% of the simulated TOA reflectances. The contribution of multiple scattering, which cannot be analytically formulated, increases significantly for $\tau = 0.3445$, composing on average 24%–42% of the outgoing radiation. Thus, using larger values of optical thickness, we cover not only the differences arising from the single-scattering component but also those associated with multiple scattering.

In comparison with MODTRAN, the optical thicknesses calculated in MODTRAN ($\tau = 0.232$ for 445 nm and $\tau = 0.097$ for 530 nm) were manually input into 6SV1. The MODTRAN atmosphere was modeled as composed of five standard gases: H_2O, CO_2, N_2O, CH_4, and O_2, with the concentrations specified by the 1976 U.S. Standard Atmosphere model requirements. We did not include O_3 into the composition to avoid the influence of absorption at 530 nm. The results are shown in Fig. 2(b). As in the case of SHARM, this comparison is characterized by excellent agreement. The maximum observed difference, calculated in reference to MODTRAN, is less than 0.085% for $\tau = 0.097$ and 0.08% for $\tau = 0.232$.

Note that the VZA range in this case is limited to 70°. As it was mentioned in Section 4, MODTRAN assumed a stratified atmosphere around a spherical Earth. To make MODTRAN applicable for the comparison with parallel atmosphere codes, we set the Earth radius to 10^{20} km and avoided using angles beyond 70°.

2. *Aerosol Atmosphere*

For an aerosol atmosphere, the performance of 6SV1 in scalar mode was tested against DISORT and MODTRAN. The atmosphere was represented by a uniform aerosol layer with a height of 2 km. The SZA and AZ geometrical conditions were the same as in the case of a molecular atmosphere. The ground surface reflectance was set to 0.

The comparison with DISORT was performed at $\lambda = 694$ nm for a standard continental aerosol model, consisting of 70% dustlike particles, 29% water-soluble particles, and 1% soot particles. The mean radius and standard deviation of each component, as reported in d'Almeida *et al.*,[32] are listed in Table 1. This type of aerosol is typical for slightly polluted regions influenced by industrial and traffic anthropogenic activities. It is characterized by a highly asymmetric scattering phase function with a strong forward-scattering peak.

The 220 Legendre coefficients and single-scattering albedo (SSA), SSA = 0.8835, as calculated in 6S, were input into DISORT. We used three different values of optical thicknesses, τ = {0.21; 0.778; 2.0}, to simulate clear, hazy, and turbid atmospheric conditions (the first two were chosen to follow the validation scheme used in the previous study[7]). For $\tau = 2.0$ we added a new VZA set where VZA varied from 3° to 78° in increments of 5°. DISORT was used as a reference in the calculation of relative percentage differences between the code outputs.

The results are presented in Fig. 3(a). There is excellent agreement between the TOA reflectances

Table 1. Parameters of Two Aerosol Models Used for the Validation of 6SV1 against the Other RT Codes

Model	Component	Percentage (by volume)	Mean Radius (μm)	Standard Deviation (μm)
Continental	Dustlike	0.70	0.471	2.512
	Water-soluble	0.29	0.0285	2.239
	Soot	0.1	0.0118	2.0
Clean maritime	Sea salt (nuclei mode)	0.538	0.05	2.03
	Sulfate	0.457	0.0695	2.03
	Sea salt (accumulation mode)	0.005	0.4	2.03

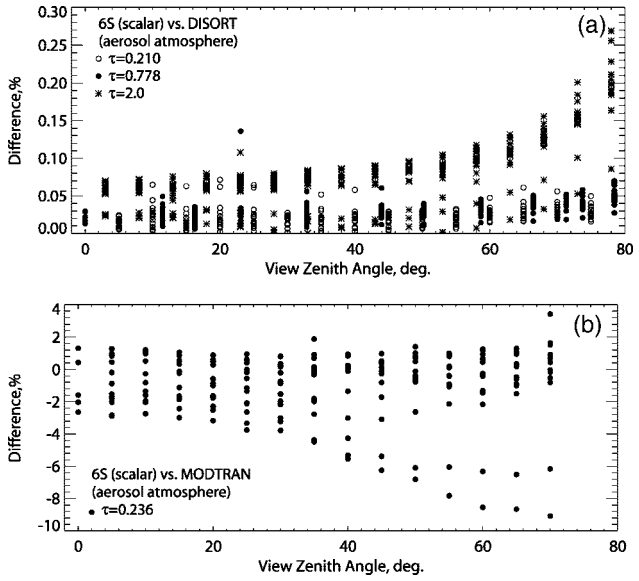

Fig. 3. Validation of 6SV1 in scalar mode against (a) DISORT and (b) MODTRAN for an aerosol atmosphere. (a) Standard continental aerosol model. SZA = {0.0°; 10.0°; 23.07°; 45.0°; 58.67°; 75.0°}, AZ = {0.0°; 90.0°; 180.0°}, VZA = {0°–79°}, optical thickness of τ = {0.210; 0.778; 2.0}, surface reflectance of ρ = 0. (b) Clean continental aerosol model. SZA and VZA sets do not include values beyond 70°, τ = 0.236, ρ = 0.

calculated by DISORT and 6SV1, which demonstrates the consistency of the two different radiative transfer methods used in the codes. The relative difference fluctuates about the zero line with a maximum deviation of less than 0.08% for τ = 0.21 and 0.778 and does not go beyond 0.28% for τ = 2.0. Multiple scattering accounts for 17%–50% of the simulated reflectances for τ = 0.21, increases significantly for τ = 0.778 (44%–72%), and becomes dominant for τ = 2.0 (69%–84%).

Note that we did not obtain an abrupt sharp reduction of accuracy as that reported in the previous study[7] for the comparison between DISORT and SHARM. In 6S and DISORT, both single- and multiple-scattering terms are calculated based on the Legendre coefficients, whereas in SHARM the single-scattering term is calculated separately based on the phase function. To compare the performance of SHARM with the performance of another RT code, one needs to supply both phase function values and Legendre coefficients. The difference between the actual phase function and the one reconstructed based on the Legendre coefficients may lead to further difference between the codes' outputs.

We also suggest that the difference of 1%–2% between the previous scalar version of 6S and SHARM, reported in the previous study,[7] was associated with the impossibility of changing the angular resolution of integration in 6S. Both DISORT and SHARM used 128 calculation (Gaussian) angles, whereas in 6S the number of calculation angles was fixed to 48, which was not enough for the case of a highly asymmetrical aerosol scattering phase function used for the comparison.

The comparison with MODTRAN was performed at λ = 550 nm for a clean continental (or rural) aerosol model, consisting of 0.01% of dustlike and 99.99% of water-soluble particles. This model refers to an aerosol type encountered in remote, pollution-free, continental areas such as nonforest savannahs and rural environments.[32] The aerosol phase function is slightly asymmetric, and 50 Legendre coefficients are generally enough to describe it thoroughly.

The results of the comparison are illustrated in Fig. 3(b). The aerosol scattering parameters and phase function, as calculated in the scalar mode of 6SV1, were input into MODTRAN. To eliminate Rayleigh scattering in MODTRAN, the atmospheric pressure was artificially reduced to 10^{-6} atm and the molecular profiles were set to 0. The relative differences between 6SV1 and MODTRAN TOA reflectances were calculated using MODTRAN as a reference. Analogously to the case of a molecular atmosphere, we did not plot the outputs for SZA and VZA beyond 70° to avoid errors associated with the conversion of a spherical atmosphere model into a linear model. We also used only one value of optical thickness, τ = 0.236, to do this comparison, and plotted the actual values of relative differences to better illustrate the difference distribution pattern.

In contrast with the excellent results of the previous comparison, MODTRAN does not demonstrate good agreement with 6SV1 for a pure aerosol atmosphere. The absolute value of relative difference varies from 0% to 9.5%. In particular, it sharply increases with the increase of VZA only for the backscattering direction (AZ = 180°, as specified in MODTRAN). For the other two relative azimuths (AZ = 0° and 90°) it generally stays within 3%. We think that this disagreement arises from the use of only 16 calculation angles (or streams) and a Henyey–Greenstein expansion for aerosol function modeling in the DISORT subroutine of MODTRAN. Even when a user-supplied function is provided, MODTRAN always models the aerosol phase function within the DISORT subroutine using a Henyey–Greenstein expansion. However, although this expansion seems to reproduce well the forward peak of Mie scattering, it usually fails to reproduce the backscattering behavior.[33]

B. Vector Mode

1. Molecular Atmosphere

For a molecular atmosphere, the performance of 6SV1 in vector mode was validated against Coulson's tabulated values and classic Monte Carlo simulations. In both cases, the atmosphere was modeled as a single molecular layer with a height of 8 km.

In the first part of comparison, the choice of geometrical and optical conditions was limited to the set of values used by Coulson *et al.*[24] We selected two values of optical thickness, 0.1 (λ = 530 nm) and 0.25 (λ = 440 nm); six values of SZA, SZA = {0.0°; 23.07°;

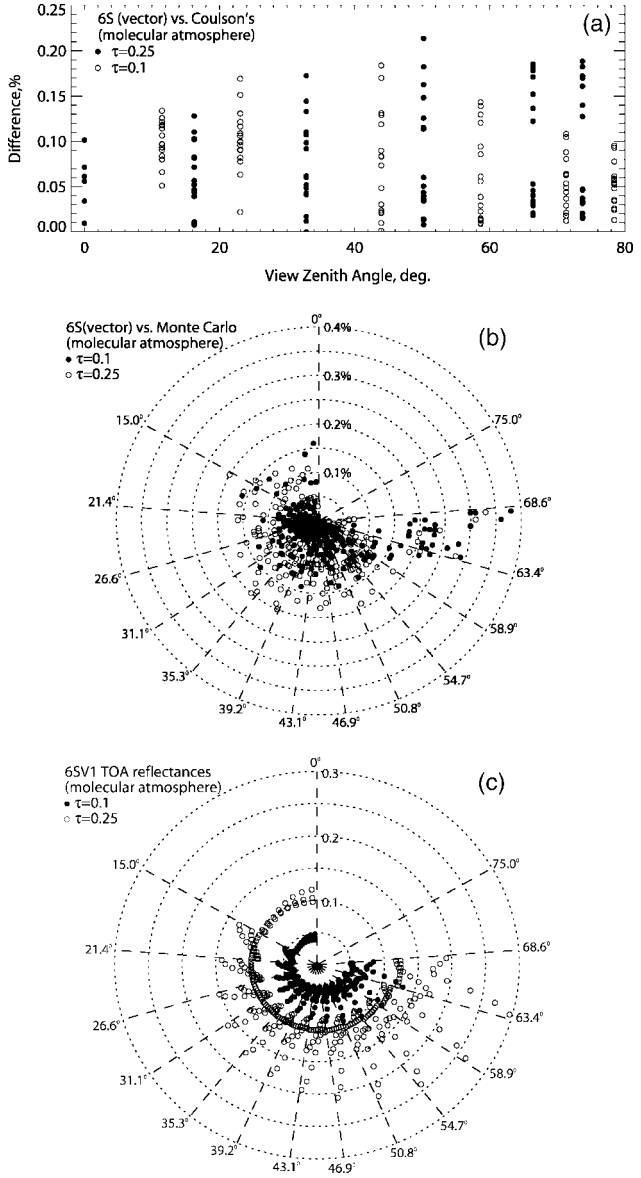

Fig. 4. (a) Validation of 6SV1 in vector mode for a molecular atmosphere against Coulson's tabulated values. SZA = {0.0°; 23.07°; 36.87°; 53.13°; 66.42°; 78.46°}, AZ = {0.0°; 90.0°; 180.0°}, VZA = {0°−79°}, τ = {0.1; 0.25}, ρ = 0. (b) Validation of 6SV1 in vector mode for a molecular atmosphere against the Monte Carlo simulations. SZA = {0.0°; 23.0°; 50.0°}, τ = {0.1; 0.25}, ρ = 0. The hemispherical space at the top of atmosphere is divided into a number of solid angles, specified by VZA and AZ values. The boundary VZA values are shown as angular coordinates. The relative difference between the outputs of the codes is presented as the radius coordinate. (c) TOA reflectances calculated by 6SV1 in vector mode for comparison with the Monte Carlo code, illustrated in (b). The reflectances are shown as the radius coordinates.

36.87°; 53.13°; 66.42°; 78.46°}; three values of relative azimuth, AZ = {0.0°; 90.0°; 180.0°}; all available values of VZA from 0° to 79°; and zero ground surface reflectivity.

The comparison was made for the three Stokes vector components: intensity of radiation I and parameters Q and U. In Coulson's tables[24] these components are presented with five-digit accuracy and as calculated in relation to incoming solar flux. To match the 6SV1 Stokes vector components, which are calculated in relation to incident radiation, we had to divide Coulson's parameters by a corresponding value of cos(SZA).

Table 2. Summary of Differences between the Stokes Parameters Q and U Calculated with 6SV1 and Extracted from Coulson's Tables[a]

Optical Thickness	SZA, (deg.)	Average Difference		Maximum Difference	
		Q	U	Q	U
0.10	0	0.00003	0.00000	0.00007	0.00000
	23.07	0.00004	0.00001	0.00009	0.00002
	36.87	0.00007	0.00001	0.00019	0.00002
	53.13	0.00003	0.00002	0.00008	0.00004
	66.42	0.00006	0.00002	0.00020	0.00004
	78.46	0.00018	0.00002	0.00061	0.00004
0.25	0	0.00014	0.00000	0.00040	0.00000
	23.07	0.00025	0.00001	0.00073	0.00002
	36.87	0.00062	0.00001	0.00179	0.00004
	53.13	0.00001	0.00002	0.00002	0.00005
	66.42	0.00010	0.00002	0.00030	0.00007
	78.46	0.00008	0.00002	0.00019	0.00009

[a]The comparison was made for SZA = {0.0°; 23.07°; 36.87°; 53.13°; 66.42°; 78.46°}, VZA = {0°–79°}, τ = {0.1°; 0.25}, ρ = 0, and AZ = {0.0°; 90.0°; 180.0°} for Q and AZ = 90.0° for U.

The results of the TOA reflectance comparison (the parameter I) are illustrated in Fig. 4(a). The overall agreement between 6SV1 and Coulson's reflectances is better than 0.22% for both values of optical thickness. The larger differences are typically observed for the backscattering direction (AZ = 180°) and the larger values of VZA. We also performed calculations for a molecular atmosphere bounded by a Lambertian surface with a reflectance of ρ = 0.25 (which are not shown here). The use of the nonzero Lambertian background led to a slight decrease of differences (down to 0.1%) between the TOA reflectances.

The results of the Q and U parameter comparison are summarized in Table 2. The summary consists of two parts: the average and the maximum differences between the calculated and extracted parameters (following the approach described in the study of Evans and Stephens[14]). For the parameter U, AZ = 0° and 180° were excluded from the comparison as U was always 0 for those angles. It should also be noted that Coulson *et al.*[24] defines Q and U with signs opposite to those used in 6SV1.

On average, the comparison is characterized by excellent agreement for the parameter U and relatively good agreement for the parameter Q. The calculated and extracted U values differ only in the fifth decimal for both optical thicknesses. The Q values also agree well for τ = 0.1, except for SZA = 78.46°, where the average difference slightly increases to 0.00018, and for three first values of SZA for τ = 0.25. The worst agreement is observed for SZA = 36.87°, with the maximum difference of 0.00179. However, this maximum difference, which made a significant contribution to the calculation of

the average difference, corresponds to VZA = 78.46°. Smaller VZA angles (within 50°) are characterized by the average difference of 0.00018.

In contrast to a simple direct comparison with Coulson's tabulated values, the validation of the 6SV1 code against Monte Carlo simulations was more time consuming and required a specific geometrical transformation of 6SV1 outputs. Instead of calculating an exact value of TOA reflectance for a given SZA–VZA–AZ configuration, the Monte Carlo program calculates the average value of all TOA reflectances confined within a given solid angle. The hemispherical space at the top of atmosphere is divided into a number of solid angles, specified by VZA and AZ values. In our case, the angular sampling for the relative AZ space (from 0° to 180°) was 22.5°. The sampling for VZA space (from 0° to 90°) is shown in Fig. 4(b). The boundary VZA values are presented as angular coordinates. The relative difference varies as the radius coordinate from 0% to 0.4%.

A special integration method was applied to match the outputs of 6SV1 and Monte Carlo. Each of the VZA (e.g., from 0° to 15°) and AZ (e.g., from 0° to 22.5°) ranges was divided into nine equal angles. 6S outputs were calculated separately at the boundaries of each angle, producing in total 100 reflectance values for one Monte Carlo solid angle. Then, the calculated 6S reflectances were integrated in zenith, using sin(VZA) as a solid angle factor, and in azimuth. Finally, the results of integration were normalized by the corresponding solid angle value.

Two values of optical thickness {0.1, 0.25} and three values of SZA {0.0°; 23.0°; 50.0°} were selected for the comparison. For each value of optical thickness, 10^{10} photons were processed. The relative differences between the code outputs, presented as open and filled circles in the plot in Fig. 4(b), were distributed uniformly within each VZA range in accordance to their AZ value. Thus, those corresponding to AZ = {0.0°–22.5°} are plotted closest to the lower VZA boundary, followed by those corresponding to AZ = {22.5°–45.0°}.

As shown in Fig. 4(b), the relative difference between the integrated TOA reflectances is a maximum for the largest values of VZA (63.4°–68.6°) and AZ (157.5°–180°). However, it still does not exceed 0.4%. For the lower VZA range, from 0° to 63.4°, the relative difference varies within 0.21%. In general, it is slightly less (within 0.17%) for the smaller value of optical thickness. The actual values of TOA reflectances, as calculated in 6SV1, are presented in Fig. 4(c).

2. *Aerosol Atmosphere*

For an aerosol atmosphere, the performance of 6SV1 in vector mode was validated against Monte Carlo simulations. The atmosphere was represented by a clean-maritime aerosol, consisting of biogenically produced sulfate (0.457%) and sea-salt particles in nuclei (0.538%) and accumulation (0.005%) modes[32] (see Table 1). This type of aerosol is produced by the oceanic areas of remote maritime environments and occurs mainly in the southern hemisphere between the equator and 60°.

The validation was performed for $\lambda = 550$ nm and two values of optical thickness, $\tau = 0.2$ and $\tau = 0.7$, used to simulate clear and hazy atmospheric conditions. The 6SV1 aerosol scattering phase function, calculated at 1000 scattering angles, was incorporated into the Monte Carlo code. The geometrical and surface configurations were the same as in the molecular case. For each value of optical thickness, 3×10^{10} photons were processed.

The obtained relative errors between the outputs of the codes are shown in Fig. 5(a). The actual values of TOA reflectances, as calculated in 6SV1, are presented in Fig. 5(b). The relative errors stay within 0.5% for VZA less than 63.4° and slightly increase (up to 0.7%) for VZA = {63.4°–68.6°}. In general, they increase further (up to 1.2%) for the next range of VZA. We did not plot these results here to provide a better picture of the relative difference pattern within the smaller VZA ranges. Moreover, the increase of difference after VZA = 68.6° can easily be neglected as it corresponds to the VZA range, which is beyond the upper-boundary VZA values (about 60°) used in MODIS data processing.

6. Effects of Polarization

A. Molecular Atmosphere

The importance of accounting for the effects of polarization in a molecular atmosphere will be demonstrated through the comparison of TOA reflectances calculated by 6SV1 in vector mode with those calculated by SHARM. The comparison was performed for the same range of optical and geometrical conditions as in scalar mode. The only difference is that 6SV1 was used as a reference this time.

The obtained results, presented in Fig. 6, show the inapplicability of a scalar RT code in the remote sensing studies that require high accuracy of RT modeling. The relative error oscillates around the zero line with the maximum observed deviation of more than 10% for $\tau = 0.3445$. The oscillation range becomes smaller with the decrease of optical thickness—it is within 5.5% for $\tau = 0.1$. A complete theoretical explanation of these large vector–scalar errors is provided in Mishchenko *et al.*[11] and need not be repeated in detail here. According to this explanation, the errors come from lower-order (except first-order) scattering paths and become more significant at the geometries involving scattering angles equal or close to 0° and 90°.

B. Aerosol Atmosphere

TOA reflectances calculated with the new version of 6S in scalar and vector modes have been compared for a biomass burning smoke aerosol model. This type of aerosol is usually produced by forest fires over the Amazonian tropical forest region in Brazil.[34] The average volume size distribution of aerosol particles, retrieved from the Aerosol Robotic Network (AERONET) measurements, is presented in Fig.

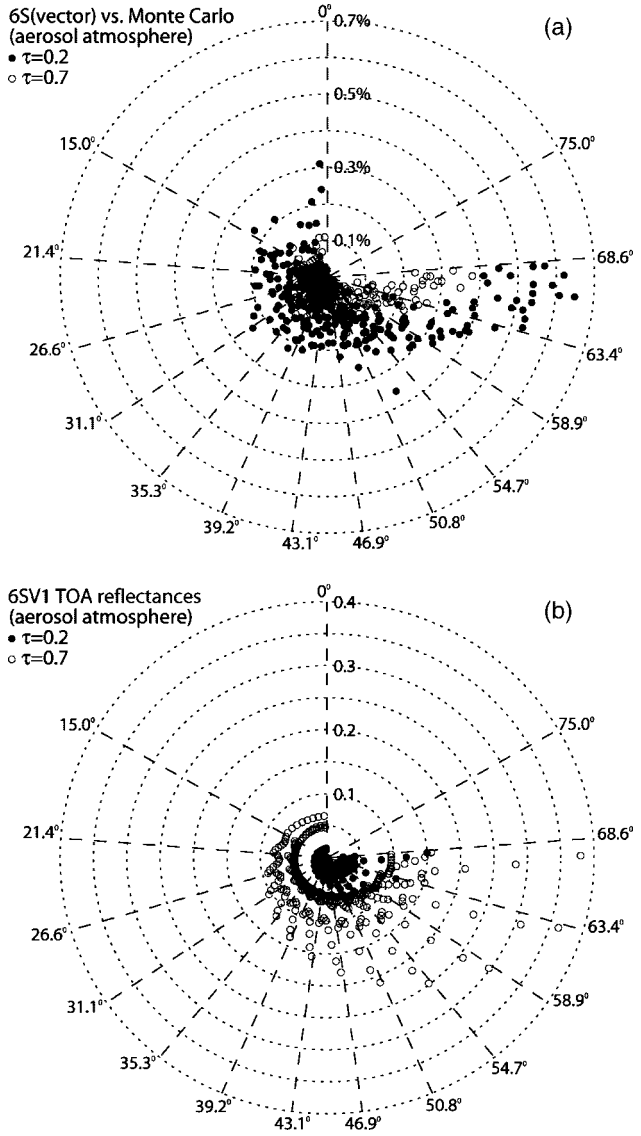

Fig. 5. (a) Validation of 6SV1 in vector mode for an aerosol atmosphere against the Monte Carlo simulations. The atmosphere is represented with the clean maritime model. SZA = {0.0°; 23.0°; 50.0°}, τ = {0.2; 0.7}, $\rho = 0$. The hemispherical space at the top of atmosphere is divided into a number of solid angles, specified by VZA and AZ values. The boundary VZA values are shown as angular coordinates. The relative difference between the outputs of the codes is presented as the radius coordinate. (b) TOA reflectances calculated by 6SV1 in vector mode for comparison with the Monte Carlo code, illustrated in Fig. 5(a). Reflectances are shown as the radius coordinates.

7(a). In the retrievals, the particles were assumed to be polydispersed homogeneous spheres with the same complex refractive index. The distribution is dominated by small particles with the mean radius of approximately 0.15 μm. SSA and the asymmetry parameter g, as calculated in 6SV1, are also specified in Fig. 7(a).

The comparison was made for two wavelengths: 470 and 670 nm. The optical thickness was fixed to 0.728 in both cases. The VZA and AZ sets of values were the same as in the comparison with DISORT. The SZA set was slightly different: SZA = {0.0°; 11.48°; 23.07°; 32.86°; 58.67°}. We used 130 Legendre coefficients to specify the aerosol scattering phase function.

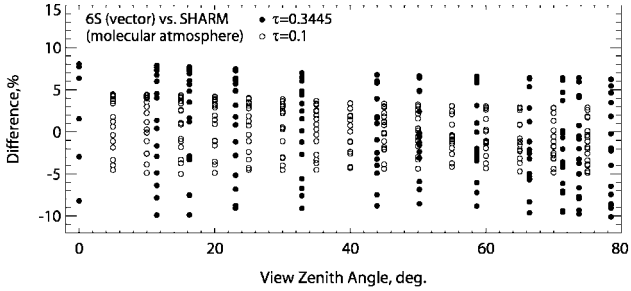

Fig. 6. Effects of polarization for a molecular atmosphere. SZA = {0.0°; 10.0°; 23.07°; 45.0°; 58.67°; 75.0°}, AZ = {0.0°; 90.0°; 180.0°}, VZA = {0°–79°}, τ = {0.1; 0.3445}, $\rho = 0$.

Figure 7(b) illustrates the results. In contrast to the case of a molecular atmosphere, the effects of polarization seem to be more significant for a longer wavelength. The absolute value of maximum relative difference reaches 5.3% for $\lambda = 670$ nm and does not exceed 1.6% for $\lambda = 470$ nm because the aerosol scattering phase function is more polarized at longer wavelengths. In general, the aerosol contribution to the polarized reflectance is approximately proportional to its phase function and optical thickness.[35] As a result, outgoing TOA radiation becomes more polarized at longer wavelengths. For example, the degree of polarization calculated for SZA = 23.07°, AZ = 0°, and VAZ = {5.0°; 25.0°; 50.0°} is 2.35, 1.18, and 4.28, respectively, for $\lambda = 670$ nm, and only 1.99, 0.74, and 2.04 for $\lambda = 470$ nm. A more detailed explanation of this matter, including diagrams of a polarized–unpolarized phase function as a function

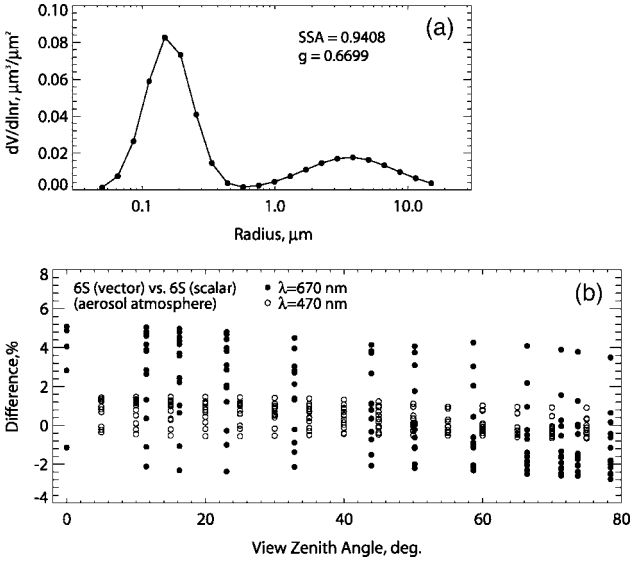

Fig. 7. (a) Average volume size distribution of particles for a biomass burning smoke aerosol model. (b) Effects of polarization for an aerosol atmosphere represented by the biomass burning smoke. SZA = {0.0°; 11.48°; 23.07°; 32.86°; 58.67°}, AZ = {0°; 90°; 180°}, VZA = {0°–79°}, $\tau = 0.728$ (hazy conditions), λ = {470; 670} nm.

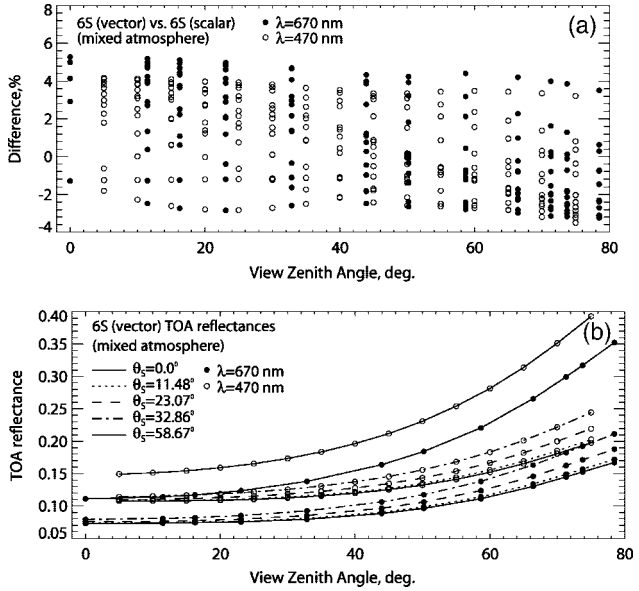

Fig. 8. (a) Effects of polarization for a mixed (molecular + aerosol) atmosphere. The aerosol constituent is represented by the biomass burning smoke model. SZA = {0.0°; 11.48°; 23.07°; 32.86°; 58.67°}, AZ = {0°; 90°; 180°}, VZA = {0°–79°}, $\tau_{aer} = 0.728$ (hazy conditions), τ mol = 0.177 for λ = 470 nm, and $\tau_{mol} = 0.042$ for λ = 670 nm. (b) TOA reflectances for the mixed atmosphere. The same geometrical conditions as in (a), except that AZ = 90°. θ_S designates SZA.

of the scattering angle, can be found in the aerosol polarized reflectance studies.[35,36]

C. Mixed Atmosphere

We have also studied the effects of polarization for the case of a mixed (aerosol + molecular) atmosphere through the comparison of simulations performed with 6SV1 in vector and scalar modes. A molecular atmosphere was added to the biomass burning smoke aerosol model used in Subsection 6.B. The total optical thickness of the molecular atmosphere, calculated in 6SV1 based on the Rayleigh law, was 0.177 for λ = 470 nm and 0.042 for λ = 670 nm.

Exponential vertical distribution profiles were assumed for both constituents. For each calculation layer, the optical thickness was calculated as

$$\tau(z) = \tau_{mol,tot} \exp(-z/H_{mol}) + \tau_{aer,tot} \exp(-z/H_{aer}), \quad (1)$$

where z is the attitude of a layer, $\tau_{mol,tot}$ and $\tau_{aer,tot}$ are the total optical thicknesses, and H_{mol} = 8 km and H_{aer} = 2 km are the total heights of the molecular and the aerosol atmospheres. The proportions of molecules and aerosol particles in each layer were calculated according to the simple mixing formulas:

$$\eta_{mol}(z) = \tau_{mol}(z)/[\tau_{mol}(z) + \tau_{aer}(z)],$$
$$\eta_{aer}(z) = \tau_{aer}(z)/[\tau_{mol}(z) + \tau_{aer}(z)]. \quad (2)$$

The relative errors between the scalar and vector simulations are presented in Fig. 8(a). The error distribution pattern at λ = 670 nm is almost the same as in the case of the pure aerosol atmosphere [see Fig. 7(b)] because the presence of the molecular component does not induce any significant extra scattering at this wavelength. However, the contribution of molecular scattering strongly increases at λ = 470 nm, leading to large differences (up to 4.3%) between the vector and scalar values. This is well illustrated by Fig. 8(b), showing the TOA reflectances calculated by 6SV1 in vector mode for AZ = 90°. Due to the strong molecular scattering, the outgoing radiation signal is larger at 470 nm than at 670 nm for all values of SZA.

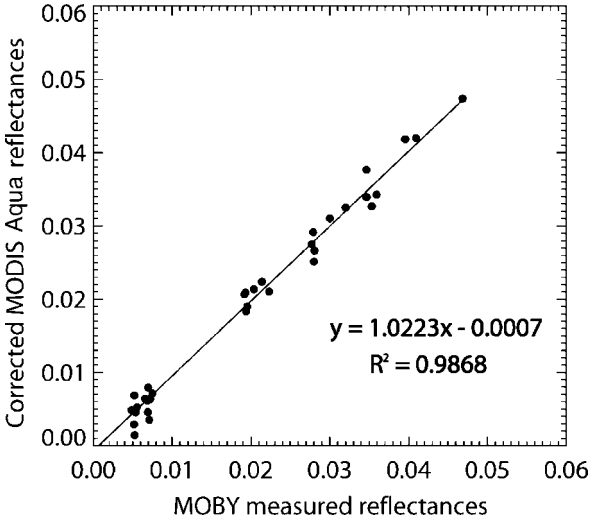

Fig. 9. Corrected MODIS Aqua water-leaving reflectances versus the MOBY-measured water-leaving reflectances for λ = {412; 443; 490; 530; 550} nm. MOBY data were collected off the coast of Lanai Island, Hawaii, during 2003.

7. Validation of the Vector 6S against Ocean Reflectance Measurements

MODIS Aqua data, collected over the Hawaiin islands, have been corrected using the new version of 6S and AERONET measurements taken at Lanai Island. The estimated water-leaving reflectances were compared with those measured by MOBY just above the ocean surface at λ = {412; 443; 490; 530; 550} nm. We carefully selected a number of cloud-free days in 2003 when MODIS, MOBY, and AERONET measurements were taken at approximately the same time. These days included 2 January, 1 February, 10 February, 3 September, 19 September, 6 October, and 22 October.

The MOBY data were obtained directly from the MOBY principal investigator.[37] MOBY is a 14 m long buoy system designed to measure upwelling radiance and downwelling irradiance at the sea surface and three deeper depths, including 1, 5, and 9 m. These data are then processed and made available to SeaWiFS (Sea-Viewing Wide Field-of-View Sensor) and MODIS ocean science teams.[38]

The AERONET data, including the optical thickness values, particle size distributions and complex refractive indices, were used as 6SV1 input parame-

ters. These data were retrieved by the new inversion code of AERONET, which works under the assumption that aerosol particles are homogeneous spheres and the index of refraction is not fixed.[39]

The 6SV1 simulations were run for an ocean BRDF scheme that accounted for sea surface anisotropy effects, foam contributions, and sunglint.[40,41] A separate correction was made to account for the instrument polarization sensitivity.[42] Thus, this comparison tests not only the path radiance computation for the case of a mixed (aerosol + molecular) atmosphere but also the adopted ocean BRDF scheme and its coupling with the atmosphere radiation field.

Figure 9 shows the results of the comparison. The agreement between the corrected MODIS and the MOBY water-leaving reflectances is 0.001 to 0.002 for the {400–550} nm region. A simple regression analysis reveals a slight underestimation (about 2%) of the corrected MODIS reflectances.

8. Conclusions

The new version of the 6S radiative transfer code (6SV1), capable of accounting for radiation polarization has been presented and validated in this study. The validation was done separately for vector and scalar modes of the code. In scalar mode, 6SV1 was tested against other recognized and widely used scalar RT codes. In vector mode, 6SV1 was validated with respect to Coulson's tabulated values, Monte Carlo code, and ocean water-leaving reflectance measurements. We also demonstrated the necessity of the accounting for radiation polarization through the comparison of vector and scalar RT simulations for different sets of geometric and atmospheric conditions.

The validation of 6SV1 in scalar mode was important for the following reasons. First, it helped resolve the questions about the accuracy of the code posed in the previous comparison studies. Second, it demonstrated the consistency of the successive orders of scattering method with other RT methods, such as discrete ordinates and spherical harmonics. Finally, the scalar mode of the code was used in the study of the effects of polarization.

The obtained results have shown that 6SV1, used in scalar mode, agrees consistently with SHARM and DISORT, with an accuracy of better than 0.08%. It also demonstrates good agreement (within 0.1%) in comparison with MODTRAN4 for a pure molecular atmosphere. Its considerable disagreement with MODTRAN4 for the case of a pure aerosol atmosphere (up to 9.5% for larger VZA values) is most probably caused by the use of a Henyey–Greenstein expansion for the aerosol function modeling and an insufficient number of calculation angles (or streams) in the DISORT subroutine of MODTRAN4. The next version of MODTRAN, which is anticipated to be released at the end of 2005, will fix the angle problem by introducing an arbitrary maximum number of streams.

The code 6SV1 has also demonstrated good performance in vector mode. It agrees well (within 0.22%) with Coulson's tabulated values for a molecular atmosphere. Its simulations are also in fairly good agreement with those of Monte Carlo: within 0.4% for a molecular atmosphere and 0.7% for an aerosol atmosphere. The MODIS Aqua water-leaving reflectances, corrected using the vector mode of 6SV1, coincide with the MOBY-measured reflectances within the range of 0.001 to 0.002 for the {400–550} nm region. The observed differences are not of concern, as they are much less than the 2% accuracy of raw MODIS TOA reflectance data.

The comparison between scalar and vector RT simulations has shown that ignoring the effects of polarization leads to large errors in calculated TOA reflectances. The maximum relative error is more than 10% for a pure molecular atmosphere and is up to 5% for a pure aerosol atmosphere. Therefore the accounting for radiation polarization is extremely important for atmospheric correction of remotely sensed data, especially those measured over dark targets, such as ocean surfaces or dark dense vegetation canopies.

Several upgrades incorporated into 6SV1 have enhanced the quality of the code performance. The user has obtained an option to control the accuracy of calculations by changing the number of calculation angles and layers, and, in the case of aerosols, the number of Legendre coefficients. However, one should not forget that variations of these parameters usually involve changes of processing (or computation) time.

Our future plans include further validation, refinement, and optimization of the code. Part II of this study would include more results of the code validation for a molecular–aerosol–mixed atmosphere with Lambertian and anisotropic surface boundaries. We will also continue our work on the retrieval of ocean water-leaving reflectances. Meanwhile, since the results of the Part I validation are quite satisfactory, 6SV1 will be used to calculate lookup tables for collection 5 of MODIS surface reflectances.

We thank F.-M. Breon for providing the Monte Carlo code, A. Lyapustin for providing SHARM, G. Anderson for providing MODTRAN, D. Clark for providing the MOBY measurements, F.-M. Breon and A. Lyapustin for multiple discussions and suggestions during this study, and the three anonymous referees for their helpful comments. This work was supported by NASA contract NNG04HZ17C.

References

1. K.-N. Liou, *An Introduction to Atmospheric Radiation* (Academic, 1980).
2. J. E. Hansen and L. D. Travis, "Light scattering in planetary atmospheres," Space Sci. Rev. **16,** 527–610 (1974).
3. J. W. Hovenier, C. van der Mee, and H. Domke, *Transfer of Polarized Light in Planetary Atmospheres: Basic Concepts and Practical Methods* (Kluwer Academic, 2004).
4. K. Stamnes, S. C. Tsay, W. Wiscombe, and K. Jayaweera, "Numerically stable algorithm for discrete-ordinate method radiative transfer in multiple scattering and emitting layered media," Appl. Opt. **27,** 2502–2509 (1988).
5. K. Stamnes, S. C. Tsay, W. Wiscombe, and I. Laszlo, "DISORT, a general-purpose FORTRAN program for Discrete-Ordinate-

Method radiative transfer in scattering and emitting layered media: documentation of methodology, version 1.1," (March, 2000), available as DISORTReport1.1.pdf at ftp://climate1.gsfc.nasa.gov/wiscombe/Multiple_Scatt/.
6. A. Berk, L. S. Bernstein, G. P. Anderson, P. K. Acharya, D. C. Robertson, J. H. Chetwynd, and S. M. Adler-Golden, "MODTRAN cloud and multiple scattering upgrades with application to AVIRIS," Remote Sens. Environ. **65,** 367–375 (1998).
7. A. Lyapustin, "Radiative transfer code SHARM-3D for radiance simulations over a non-Lambertian nonhomogeneous surface: intercomparison study," Appl. Opt. **41,** 5607–5615 (2002).
8. J.-L. Roujean, M. Leroy, and P.-Y. Dechamps, "A bidirectional reflectance model of the Earth's surface for the correction of remote sensing data," J. Geophys. Res. **97D,** 20455–20468 (1992).
9. A. Lyapustin, D. L. Williams, B. Markham, J. Irons, B. Holben, and Y. Wang, "A method for unbiased high-resolution aerosol retrieval from Landsat," J. Atmos. Sci. **61,** 1233–1244 (2004).
10. H. C. van de Hulst, *Multiple Light Scattering* (Academic, 1980).
11. M. I. Mishchenko, A. A. Lacis, and L. D. Travis, "Errors induced by the neglect of polarization in radiance calculations for Rayleigh-scattering atmospheres," J. Quant. Spectrosc. Radiat. Transfer **51,** 491–510 (1994).
12. A. A. Lacis, J. Chowdhary, M. I. Mishchenko, and B. Cairns, "Modeling errors in diffuse-sky radiation: vector versus scalar treatment," J. Geophys. Res. **25,** 135–138 (1998).
13. D. J. Diner, W. A. Abdou, H. R. Gordon, R. A. Kahn, Y. Knyazikhin, J. V. Martonchik, D. McDonald, S. McMuldroch, R. Myneni, and R. A. West, *MISR Level 2 Ancillary Products and Datasets Algorithm Theoretical Basis,* NASA EOS-MISR Document JPL D-13402, Rev. B (NASA JPL, 1999).
14. F. F. Evans and G. L. Stephens, "A new polarized atmospheric radiative transfer model," J. Quant. Spectrosc. Radiat. Transfer **5,** 413–423 (1991).
15. F.-M Bréon, "Reflectance of broken cloud fields: simulation and parameterization," J. Atmos. Sci. **49,** 1221–1232 (1992).
16. M. I. Mishchenko and L. D. Travis, "Satellite retrieval of aerosol properties over the ocean using polarization as well as intensity of reflected sunlight," J. Geophys. Res. **102(D14),** 16989–17013 (1997).
17. M. I. Mishchenko, B. Cairns, J. E. Hansen, L. D. Travis, R. Burg, Y. J. Kaufman, J. V. Martins, and E. P. Shettle, "Monitoring of aerosol forcing of climate from space: analysis of measurements requirements," J. Quant. Spectrosc. Radiat. Transfer **88,** 149–161 (2004).
18. H. R. Gordon and D. J. Castaño, "Coastal zone color scanner atmospheric correction algorithm: multiple scattering effects," Appl. Opt. **26,** 2111–2122 (1987).
19. Y. Wang, Y. Tian, Y. Zhang, N. El-Saleous, Y. Knyazikhin, E. Vermote, and R. B. Myneni, "Investigation of product accuracy as a function of input and model uncertainties: case study with SeaWiFS and MODIS LAI/FPAR algorithm," Remote Sens. Environ. **78,** 299–313 (2001).
20. F. A. Heinsch, M. Reeves, C. F. Bowker, P. Votava, S. Kang, C. Milesi, M. Zhao, J. Galssy, W. M. Jolly, J. S. Kimball, R. R. Nemani, and S. W. Running, "User's Guide, GPP and NPP (MOD17A2/A3), NASA MODIS Land Algorithm, Version 1.2," www.ntsg.umt.edu/modis/MOD17UsersGuide.pdf (2003).
21. E. F. Vermote, N. Z. El Saleous, C. O. Justice, Y. J. Kaufman, J. Privette, L. Remer, J.-C. Roger, and D. Tanré, "Atmospheric correction of visible to middle infrared EOS-MODIS data over land surface, background, operational algorithm and validation," J. Geophys. Res. **102,** 17131–17141 (1997).
22. E. F. Vermote, N. Z. El Saleous, and C. O. Justice, "Atmospheric correction of MODIS data in the visible to middle infrared: first results," Remote Sens. Environ. **83,** 97–111 (2002).
23. E. F. Vermote, D. Tanré, J. L. Deuzé, M. Herman, and J. J. Morcrette, "Second simulation of the satellite signal in the solar spectrum, 6S: an overview," IEEE Trans. Geosci. Remote Sens. **35,** 675–686 (1997).
24. K. L. Coulson, J. V. Dave, and Z. Sekera, *Tables Related to Radiation Emerging from a Planetary Atmosphere with Rayleigh Scattering* (U. California Press, 1960).
25. J. E. Hansen, "Circular polarization of sunlight reflected by clouds," J. Atmos. Sci. **28,** 1515–1516 (1971).
26. J. Lenoble, ed., *Radiative Transfer in Scattering and Absorbing Atmospheres: Standard Computational Procedures* (A. Deepak Publishing, 1985).
27. S. Chandrasekhar, "Foreword," in *Tables Related to Radiation Emerging from a Planetary Atmosphere with Rayleigh Scattering,* K. L. Coulson, J. V. Dave, and Z. Sekera, (U. of California Press, 1960).
28. T. Z. Muldashev, A. I. Lyapustin, and U. M. Sultangazin, "Spherical harmonics method in the problem of radiative transfer in the atmosphere–surface system," J. Quant. Spectrosc. Radiat. Transfer **61,** 393–404 (1998).
29. K. F. Evans, "The spherical harmonics discrete ordinate method for three-dimensional atmospheric radiative transfer," J. Atmos. Sci. **55,** 429–446 (1998).
30. A. Berk, G. P. Anderson, L. S. Bernstein, P. K. Acharya, H. Dothe, M. W. Matthew, S. M. Adler-Golden, J. H. Chetwynd, Jr., S. C. Richtsmeier, B. Pukall, C. L. Allred, L. S. Jeong, and M. L. Hoke, "MODTRAN4 radiative transfer modeling for atmospheric correction," in *Optical Spectroscopic Techniques and Instrumentation for Atmospheric and Space Research III,* Proc. SPIE **3756,** 348–353 (1999).
31. P. K. Acharya, A. Berk, G. P. Anderson, N. F. Larsen, S.-C. Tsay, and K. H. Stamnes, "MODTRAN4: multiple scattering and bi-directional reflectance distribution function (BRDF) upgrades to MODTRAN," in *Optical Spectroscopic Techniques and Instrumentation for Atmospheric and Space Research III,* Proc. SPIE **3756,** 354–362 (1999).
32. G. A. d'Almeida, P. Koepke, and E. P. Shettle, *Atmospheric Aerosols: Global Climatology and Radiative Characteristics* (A. Deepak Publishing, 1991).
33. D. Toublanc, "Henyey–Greenstein and Mie phase functions in Monte Carlo radiative transfer computations," Appl. Opt. **35,** 3270–3274 (1996).
34. O. Dubovik, B. Holben, T. F. Eck, A. Smimov, Y. J. Kaufman, M. D. King, D. Tanré, and I. Slutsker, "Variability of absorption and optical properties of key aerosol types observed in worldwide locations," J. Atmos. Sci. **59,** 590–608 (2002).
35. F.-M. Bréon, J.-L. Deuzé, D. Tanré, and M. Herman, "Validation of spaceborne estimates of aerosol loading from Sun photometer measurements with emphasis on polarization," J. Geophys. Res. **102,** 17187–17196 (1997).
36. M. Herman, J.-L. Deuzé, C. Devaux, P. Goloub, F.-M. Bréon, and D. Tanré, "Remote sensing of aerosols over land surfaces including polarization measurements and application to POLDER measurements," J. Geophys. Res. **102,** 17039–17050 (1997).
37. D. Clark, MOBY principal investigator, Ocean Science Team Member (personal communication), http://modis.gsfc.nasa.gov/sci_team/directory/.
38. D. K. Clark, M. E. Feinholz, M. A. Yarbrough, B. C. Johnson, S. W. Brown, Y. S. Kim, and R. A. Barnes, "An overview of the radiometric calibration of MOBY," in *Earth Observing Systems VI,* Proc. SPIE **4483,** 64–76 (2002).

39. O. Dubovik and M. D. King, "A flexible inversion algorithm for retrieval of aerosol optical properties from Sun and sky radiance measurements," J. Geophys. Res. **105,** 20673–20696 (2000).
40. P. Koepke, "Effective reflectance of oceanic whitecaps," Appl. Opt. **23,** 1816–1824 (1984).
41. D. Tanre, M. Herman, and P. Y. Deschamps, "Influence of the atmosphere on space measurements of directional properties," Appl. Opt. **22,** 733–741 (1983).
42. G. Meister, E. J. Kwiatkowska, B. A. Franz, F. S. Patt, G. C. Feldman, and C. R. McClain, "Moderate resolution imaging spectroradiometer ocean color polarization correction," Appl. Opt. **44,** 5524–5535 (2005).